

# First-principles investigation of $\text{Nd}(\text{Fe},\text{M})_{12}$ ( $\text{M} = \text{K}-\text{Br}$ ) and $\text{Nd}(\text{Fe},\text{Cr},\text{Co},\text{Ni},\text{Ge},\text{As})_{12}$ : Possible enhancers of Curie temperature for $\text{NdFe}_{12}$ magnetic compounds

Taro Fukazawa,<sup>1,\*</sup> Hisazumi Akai,<sup>2,3</sup> Yosuke Harashima,<sup>1,3,4</sup> and Takashi Miyake<sup>1,3</sup>

<sup>1</sup>*CD-FMat, National Institute of Advanced Industrial Science and Technology, Tsukuba, Ibaraki 305-8568, Japan*

<sup>2</sup>*The Institute for Solid State Physics, The University of Tokyo, Kashiwa, Chiba 277-8581, Japan*

<sup>3</sup>*ESICMM, National Institute for Materials Science, Tsukuba, Ibaraki 305-0047, Japan*

<sup>4</sup>*Center for Computational Sciences, University of Tsukuba, Tsukuba, Ibaraki 305-8577, Japan*

(Dated: August 18, 2021)

We investigate the effects of various dopants ( $M = \text{K}-\text{Br}$ ) on the Curie temperature of the magnetic compound  $\text{NdFe}_{12}$  through first-principles calculations. Analysis by the Korringa–Kohn–Rostoker method with the coherent potential approximation reveals that doping the Fe sites with optimal concentrations of Ge and As is a promising strategy for increasing the Curie temperature. To search over a wider space, we also perform Bayesian optimization. Out of over 180,000 candidate compositions, co-doped systems with Co, Ge, and As are found to have the highest Curie temperatures.

PACS numbers: TBD

Keywords: TBD

## I. INTRODUCTION

Rare-earth–iron compounds are used in the highest-performance permanent magnets currently available. The magnetic compound  $\text{Nd}_2\text{Fe}_{14}\text{B}$  is especially well known as the main phase of neodymium magnets, which are the strongest magnets used industrially. In such magnets, rare-earth elements are the main source of the magnetic anisotropy and iron is the main source of the magnetic moment.

Compounds with the  $\text{ThMn}_{12}$  structure are considered promising because they can accommodate a larger amount of Fe than  $\text{Nd}_2\text{Fe}_{14}\text{B}$ . Hirayama et al. synthesized films of  $\text{NdFe}_{12}$  and reported that the nitrogenated film exhibited larger magnetization and higher Curie temperature than  $\text{Nd}_2\text{Fe}_{14}\text{B}$ .<sup>[1, 2]</sup> However,  $\text{NdFe}_{12}(\text{N})$  is not thermodynamically stable.

Doping of  $R\text{Fe}_{12}$  has been investigated as a method for stabilizing the structure as a bulk material and enhancing the magnetic properties. Optimization of the material properties by changing the composition of the system is one of the central issues in the field.

Titanium energetically stabilizes the structure, and an Fe-rich magnetic compound with a  $\text{ThMn}_{12}$ -type structure was first found as a Ti-doped system.<sup>[3, 4]</sup> However, Ti also greatly reduces the magnetization of the system owing to its antiferromagnetic coupling to the host Fe.<sup>[5]</sup> Cobalt is a typical enhancer of finite-temperature magnetism. With respect to  $\text{ThMn}_{12}$  compounds, Hirayama et al. reported the synthesis of Co-doped  $\text{Sm}(\text{Fe},\text{Co})_{12}$  films that displayed excellent magnetic properties at room temperature and a higher Curie temperature than the pristine system.<sup>[6]</sup> First-principles calculations have

suggested that Co not only improves the magnetic properties but also contributes to the stability of the  $\text{ThMn}_{12}$  structure.<sup>[5]</sup> We also discussed the enhancement of the Curie temperature,  $T_C$ , and demonstrated that Cr is a better enhancer of this parameter than Co in  $R\text{Fe}_{12}$  ( $R=\text{Y}, \text{Nd}, \text{Sm}$ ) when the dopant concentration is low.<sup>[7]</sup> Using V, which is adjacent to Cr in the periodic table, Schönhöbel et al. synthesized  $\text{SmFe}_{11}\text{V}$  and reported that its Curie temperature was 635 K,<sup>[8]</sup> which is significantly higher than the value of 555 K for  $\text{SmFe}_{12}$ .<sup>[6]</sup>

These works motivated us to explore a wider composition space for  $T_C$ -enhancing dopants. We have recently developed a Bayesian optimization framework for such exploration and demonstrated that it can greatly reduce the number of first-principles calculations required to identify the optimal system from a large candidate set.<sup>[9]</sup> However, we considered only a few dopant elements in our previous study. In this paper, we examine a series of dopants, namely,  $M = \text{K}, \text{Ca}, \text{Sc}, \text{Ti}, \text{V}, \text{Cr}, \text{Mn}, \text{Co}, \text{Ni}, \text{Cu}, \text{Zn}, \text{Ga}, \text{Ge}, \text{As}, \text{Se},$  and  $\text{Br}$ , as potential enhancers of the Curie temperature through first-principles calculations and also consider co-doping with some of these elements.

In Section II, we describe the details of the calculations. As the first step, we performed first-principles calculations of  $\text{NdFe}_{12-\delta}\text{M}_\delta$  for all of the dopants in the dilute limit of  $M$  ( $\delta \ll 1$ ). In Section III A, we discuss how the dopants affect the Curie temperature. On the basis of the results, we selected six dopants (V, Cr, Co, Ni, Ge, and As) with the potential to enhance the Curie temperature, and we examine how a single dopant changes the Curie temperature at a finite concentration in Section III B. We also consider the effects of Ge and As as dopants on the Curie temperature in terms of hybridization between the Fe 3d and  $M$  4p orbitals.

In Section III C, we consider the case of multiple dopants and report on their advantages over a single

\* E-mail: taro.fukazawa@aist.go.jp

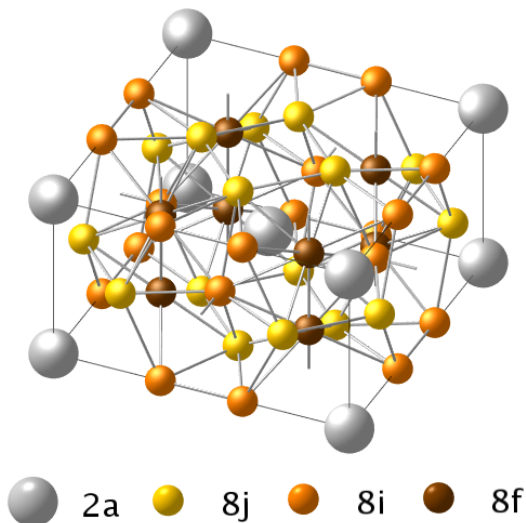


FIG. 1. Structure of a ThMn<sub>12</sub>-type crystal and its Wyckoff positions.

dopant. In the case of co-doping, the number of possible combinations becomes very large. To deal with this difficulty, we applied the Bayesian optimization framework that we proposed previously.[9] We demonstrate that co-doping with Co, Ge, and As has an advantage over doping with Co alone. Finally, we present our conclusions in Section IV.

## II. METHODS

We performed first-principles electronic structure calculations based on density functional theory.[10, 11] We used the Korringa–Kohn–Rostoker[12, 13] (KKR) Green’s function method to solve the Kohn–Sham equations and the local density approximation for the exchange–correlation functional. Although the spin–orbit coupling was not explicitly included in the energy functional, the electronic configuration of the f electrons at the Nd site was assumed to obey Hund’s rule. The f electrons were treated with the open-core approximation and the self-interaction correction[14] was applied to the f states. The randomness due to the occupation of dopants was treated within the coherent potential approximation (CPA).[15–17]

We assumed that NdFe<sub>12</sub> possesses the crystal structure of ThMn<sub>12</sub> [space group: I4/mmm (#139)] (Fig. 1), and we adopted the lattice constant of NdFe<sub>12</sub> previously obtained [18] for undoped and doped systems.

The Curie temperature was calculated from a classical Heisenberg model whose parameters were determined using Liechtenstein’s method [19] within the mean-field approximation. Although this method overestimates the Curie temperature, the relative changes among Fe-rich magnetic compounds are adequately described.[20] Read-

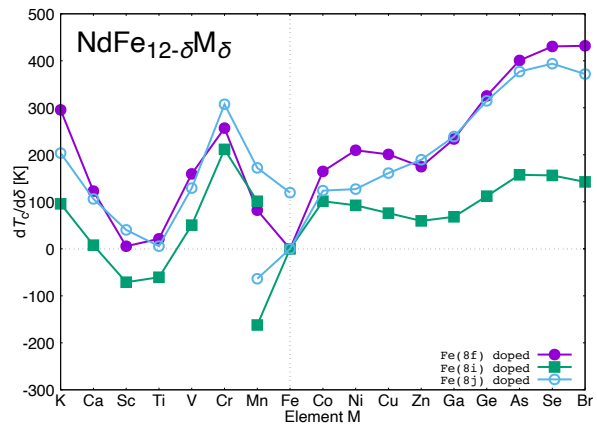


FIG. 2. Derivative of the Curie temperature for Nd(Fe<sub>12-δ</sub>M<sub>δ</sub>) with respect to  $\delta$  in the dilute limit,  $\delta \rightarrow 0$ . These values are the sum of the direct contribution shown in Fig. 3 and the indirect contribution shown in Fig. 4.

ers are referred to Ref. 7 for the details of the calculations.

We considered the doping of the Fe(8f), Fe(8i), and Fe(8j) sites in NdFe<sub>12</sub>. The magnetic moment of the dopant  $M$  was assumed to be parallel or antiparallel to the total magnetic moment of the system. Thus, we performed calculations with the initial magnetic moment of the dopant set parallel and antiparallel and carefully checked for the existence of metastable states. The results for NdFe<sub>12-δ</sub>M<sub>δ</sub> at an infinitesimal concentration (i.e., the dilute limit:  $\delta \ll 1$ ) were obtained by fitting the data for  $\delta = 0, 0.04, 0.08, 0.12$ , and  $0.16$  with polynomial curves. The derivatives of the physical quantities are calculated from the results.

To consider the case of co-doping with multiple elements, we used a Bayesian framework for composition optimization to identify the optimal system from a large search space. The search framework was previously described in Ref. 9. For the Bayesian optimization, we used the COMBO package, which can accommodate a large number of candidates.[21, 22] The choice of system to explore next was conducted by Thompson sampling after the initial 20 systems had been chosen at random. The dimensionality of the random feature maps was set to 2000.

## III. RESULTS AND DISCUSSION

### A. NdFe<sub>12-δ</sub>M<sub>δ</sub> ( $\delta \ll 1$ )

In this subsection, we present the results for NdFe<sub>12-δ</sub>M<sub>δ</sub> in the dilute limit of  $M$  ( $\delta \ll 1$ ). Figure 2 shows the derivative of  $T_C$  with respect to concentration,  $\frac{dT_C}{d\delta} \Big|_{\delta=0}$ . In a previous paper,[7] we demonstrated the potential of Cr in enhancing the Curie temperature of  $R$ Fe<sub>12</sub> ( $R=Y, Nd, Sm$ ) more efficiently than Co for low dopant concentrations. The curve of the derivative

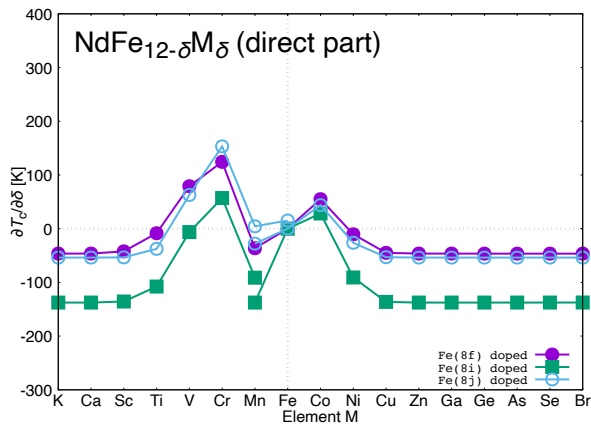


FIG. 3. Direct contribution to the derivative of the Curie temperature for  $\text{Nd}(\text{Fe}_{12-\delta}\text{M}_{\delta})$  in the dilute limit.

shown in the figure exhibits a peak at  $M=\text{Cr}$ . We also see that there are significant increases for both  $M=\text{K}$  and  $M=\text{Ge}-\text{Br}$ .

To analyze the origin of the enhancement, we performed direct-indirect decomposition (DID), which we previously proposed.[7] The Curie temperature can be calculated from the intersite couplings  $J_{ij}$  and concentration  $\delta$  within the mean-field approximation. Because  $J_{ij}$  is also a function of  $\delta$ , we see that the change of  $T_C$  with respect to concentration can be expressed as

$$\left. \frac{dT_C[\{J_{ij}(\delta)\}, \delta]}{d\delta} \right|_{\delta=0} = \left. \frac{\partial T_C}{\partial \delta} \right|_{\{J_{ij}(0)\}} + \sum_{ij} \left. \frac{\partial T_C}{\partial J_{ij}} \frac{dJ_{ij}}{d\delta} \right|_{\delta=0}. \quad (1)$$

The first and second terms are referred to as the direct and indirect parts, respectively.

Figure 3 shows the direct contribution to the derivative of  $T_C$ , which originates from the difference in the magnetic couplings between the replacing Fe- $M$  couplings and the replaced Fe-Fe couplings. The direct contribution is largely positive for  $M = \text{Co}$ ,  $\text{Cr}$ , and  $\text{V}$ , whereas it is negative for most of the remaining cases.

Figure 4 shows the indirect contribution obtained from the DID, which originates from the enhancement of the magnetic Fe-Fe couplings due to the introduction of  $M$ . It is noteworthy that the significant enhancement observed for  $M=\text{K}$  and  $\text{Ge}-\text{Br}$  in Fig. 2 can be attributed solely to the indirect contribution. We discuss the atomic-scale origin of this enhancement in terms of hybridization between the Fe 3d and  $M$  4p orbitals in the next subsection.

To roughly estimate the Curie temperature for finite dopant concentrations, we constructed a quadratic model of  $T_C$  as a function of the concentration through estimation of the first and second derivatives by data fitting:

$$T_C(\delta) = T_C(0) + \frac{dT_C}{d\delta}(0)\delta + \frac{1}{2} \frac{d^2T_C}{d\delta^2}(0)\delta^2. \quad (2)$$

This model is valid for low dopant concentrations. Fig-

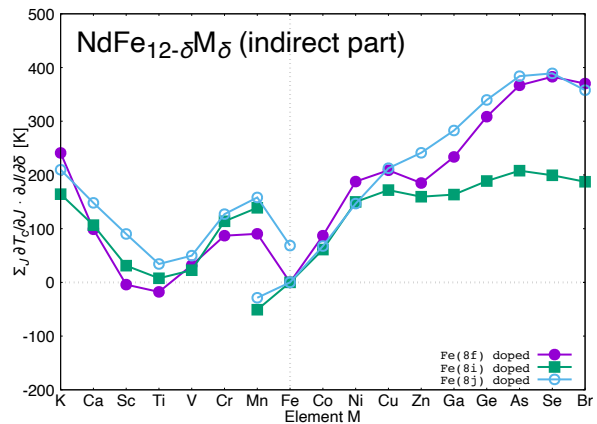


FIG. 4. Indirect contribution to the derivative of the Curie temperature for  $\text{Nd}(\text{Fe}_{12-\delta}\text{M}_{\delta})$  in the dilute limit.

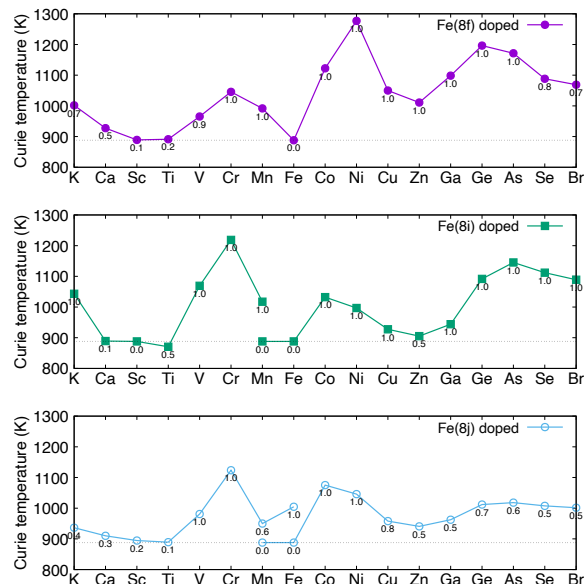


FIG. 5. Estimated maximum Curie temperatures for  $\text{Nd}(\text{Fe}_{12-\delta}\text{M}_{\delta})$  in the range of  $0 \leq \delta \leq 1$  obtained from the quadratic model. The numbers below each data point indicate the corresponding values of  $\delta$ .

ure 5 presents the highest values of  $T_C$  for  $\text{Nd}(\text{Fe}_{12-\delta}\text{M}_{\delta})$  in the range of  $0 \leq \delta \leq 1$  as a function of  $M$ . The numbers below each data point indicate the concentrations that afforded the highest values of  $T_C$ . From the figure, we can expect a large enhancement of the Curie temperature by doping with  $M = \text{V}$ ,  $\text{Cr}$ ,  $\text{Co}$ ,  $\text{Ni}$ ,  $\text{Ge}$ , or  $\text{As}$  alone.

## B. Finite amount of $M$

In this subsection, we investigate the Curie temperature of  $\text{Nd}(\text{Fe}_{12-x}\text{M}_x)$  for a finite concentration  $x$  (we let

$x$  denote the concentration to indicate that it is finite). First, we consider the results for  $M = \text{V, Cr, Co, Ni, Ge, and As}$  (which we selected on the basis of Fig. 5) to examine the validity of the rough estimation described above. To obtain the data, we performed calculations for finite concentrations of  $x = 0, 0.25, \dots, 2$ .

Figure 6 shows the calculated values of the Curie temperature. It follows from this figure that the maximum  $T_C$  was overestimated by the results shown in Fig. 5; however, the relative changes among the dopants are described well. For V and Cr,  $T_C$  begins to decrease around  $x = 1$ . In the case of Co, the maximum  $T_C$  occurs outside the range of the figure. Ni is less favorable for maintaining  $T_C$ . Ge and As display similar curves, where the maximum values of  $T_C$  occur at a higher concentration than those observed for V and Cr.

As we have previously reported,[7] Cr is a better enhancer of  $T_C$  than Co for low dopant concentrations. This is attributable to the strong antiferromagnetic Fe–Cr coupling, which leads to the direct contribution shown in Fig. 3. Vanadium plays a similar role owing to the strong Fe–V coupling, although it is less effective than Cr. In the case of Cr or V doping, the second-order effects of  $x$  decrease the Curie temperature and cause the curve to first increase and then decrease.

For  $M=\text{Co}$  or Ni, the dopants largely reinforce the magnetic Fe–Fe couplings,[7] which is the indirect contribution. The second-order effects are weak because the moment of  $M$  is parallel to the host and the  $M$ – $M$  coupling is ferromagnetic. Therefore, Co and Ni can serve as enhancers of  $T_C$  over a wider range of concentrations.

In the cases of  $M=\text{Ge}$  and As, the enhancement of the Curie temperature can be ascribed to the indirect contribution as shown in Fig. 4. This effect can be explained in terms of hybridization between the Fe 3d and  $M$  4p states. It is also noteworthy that the maxima for  $M=\text{Ge}$  and As occur at higher concentrations than for V and Cr and lower concentrations than for Co and Ni because Ge and As are non-magnetic dopants.

To examine the chemical trends, we performed calculations for 8f-doped  $\text{Nd}(\text{Fe}_{11}M)$  with  $M=\text{Ge, As, Se, and Br}$  (atomic numbers 32–35). Figure 7 shows the partial densities of states (DOSs). In the case of  $M=\text{Ge}$ , we can see from the DOS for the  $M$  p orbitals that a large part of the antibonding states remains unoccupied. This situation is comparable to *cobaltization*, in which the DOS of Fe is deformed to become similar to that of Co by hybridization with unoccupied states at a neighboring site.[23–25] This is considered to reinforce the magnetism by strengthening the magnetic coupling between the Co-like Fe and the surrounding Fe.

Upon increasing the atomic number of the dopant from  $M=\text{Ge}$ , the potential becomes deeper and more majority-spin channels are occupied (Fig. 7), while the minority-spin channels remain unoccupied. This enhances the local moment of the Fe sites (Fig. 8) and makes the spin-rotational perturbation considered in Liechtenstein’s formula larger, which increases the estimated values of the

intersite magnetic couplings and the Curie temperature. However, the *cobaltization* is simultaneously weakened by the partial occupation of the antibonding states, which decreases the Curie temperature. The crossover of these two effects is responsible for the peak in  $T_C$  for  $M=\text{As}$  observed in Fig. 9, although the local moments of Fe monotonically increase with increasing atomic number (Fig. 8).

### C. Systems with multiple dopants

Finally, we consider the co-doping of  $\text{NdFe}_{12}$  to enhance the Curie temperature. It should be readily apparent that the investigation of all possible combinations of  $M=\text{K–Br}$  would be impractical. We avoided this problem by screening the dopants on the basis of the results shown in Fig. 5; we hereinafter consider doping with Co, Ni, Ge, and As for the 8f site, Cr and Co for the 8i site, and Cr, Co, and Ni for the 8j site.

We also focus on the regime of low dopant concentrations because Fe-rich compounds are favorable in terms of magnetization, and several of the dopants were expected to afford  $T_C$  maxima at low concentrations in the range of  $x \leq 2$  (Fig. 6). We prepared two lists of candidates, lists (A) and (B), with different upper limits of dopant concentration. In list (A), the amount of each dopant per formula was varied from 0 to 1 in intervals of 0.1 with the constraint that the total amount of dopants was  $x \leq 1$ . In list (B), the amount of each dopant was varied from 0 to 2 in intervals of 0.2 with the constraint of  $x \leq 2$ . Each list consisted of 92,378 systems and up to nine site–dopant combinations per system. The total number of unique items is 182754 (2002 duplicates).

Even with this screening, considerable time and resources would be required to perform first-principles calculations for all of the candidates. To overcome this problem, we applied our efficient framework for optimization of the chemical composition based on Bayesian optimization.[9] With this framework, it is possible to identify high-performance materials from a candidate list with a small number of data acquisition processes by alternately performing data acquisition and stochastic modeling.

Figure 10 shows the obtained Curie temperature versus the number of data acquisition steps. In these plots, the score ( $T_C$ ) at each step and cumulative best score are shown for lists (A) and (B). In both cases, the best system observed during the run was found within the first 60 steps. After this point, the score oscillated between lower values, indicating that there remained few or no better systems.

The ten best identified systems are shown in Table I for list (A) and Table II for list (B). All of the top ten systems contain the maximal amount of dopants, namely,  $x = 1$  for list (A) and  $x = 2$  for list (B). For list (A), doping with As and Ge give high scores than doping with Co. For list (B), which could accommodate more dopant

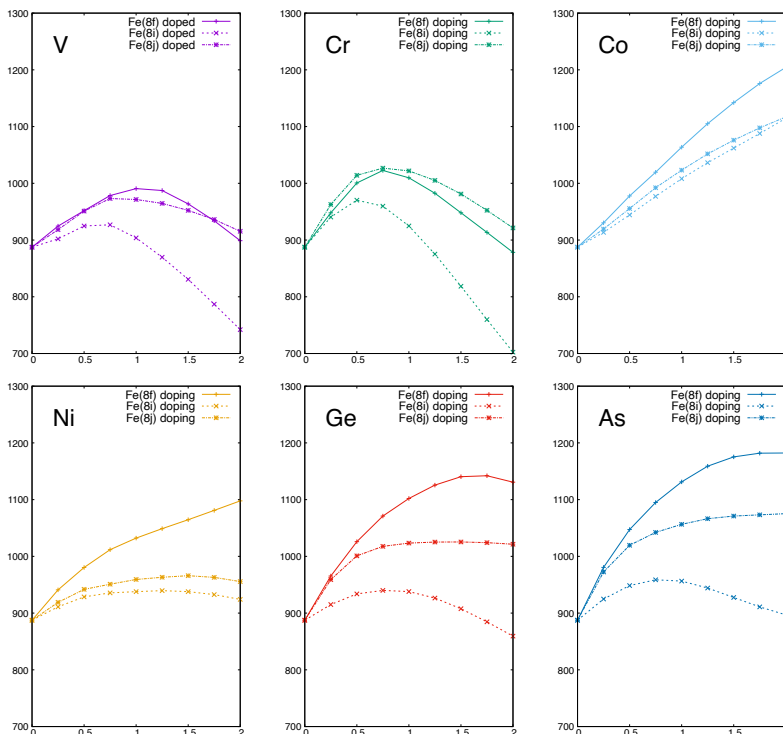


FIG. 6. Curie temperatures for  $\text{Nd}(\text{Fe}_{12-x}\text{M}_x)$  ( $M=\text{V}, \text{Cr}, \text{Co}, \text{Ni}, \text{Ge}, \text{or As}$ ) with finite concentrations  $x$  in the range of  $0 \leq x \leq 2$ .

TABLE I. Ten best systems found in the optimization using list (A).

Formula	$T_C$ (K)	$\mu_0 M$ (T)
$\text{NdFe}_{11}\text{As}$	1119	1.58
$\text{NdFe}_{11}\text{As}_{0.9}\text{Ge}_{0.1}$	1117	1.58
$\text{NdFe}_{11}\text{As}_{0.8}\text{Ge}_{0.2}$	1114	1.58
$\text{NdFe}_{11}\text{As}_{0.9}\text{Co}(8j)_{0.1}$	1112	1.60
$\text{NdFe}_{11}\text{As}_{0.8}\text{Co}(8f)_{0.2}$	1111	1.61
$\text{NdFe}_{11}\text{As}_{0.7}\text{Ge}_{0.3}$	1111	1.58
$\text{NdFe}_{11}\text{As}_{0.7}\text{Ge}_{0.2}\text{Co}(8f)_{0.1}$	1109	1.60
$\text{NdFe}_{11}\text{As}_{0.7}\text{Ge}_{0.1}\text{Co}(8f)_{0.2}$	1108	1.61
$\text{NdFe}_{11}\text{As}_{0.8}\text{Ge}_{0.1}\text{Co}(8i)_{0.1}$	1108	1.59
$\text{NdFe}_{11}\text{As}_{0.6}\text{Ge}_{0.4}$	1108	1.58
$\text{NdFe}_{12}$	881	1.73

atoms, doping with Co was more advantageous. However, the system with the highest Curie temperature was obtained by co-doping with As and Co. From comparison of  $\text{NdFe}_{10}\text{Co}(8f)_{1.8}\text{As}_{0.2}$  and  $\text{NdFe}_{10}\text{Co}(8f)_2$ , the direct and indirect contributions of As to the enhancement of  $T_C$  can be estimated as  $-22$  and  $+24$  K, respectively. Arsenic enhances the magnetic couplings between surrounding transition metals, and this effect is evidently slightly larger than that of the loss of the Co-Fe and Co-Co couplings resulting from the substitution. It is also noteworthy that substitution with Ge and As can

TABLE II. Ten best systems found in the optimization using list (B).

Formula	$T_C$ (K)	$\mu_0 M$ (T)
$\text{NdFe}_{10}\text{Co}(8f)_{1.8}\text{As}_{0.2}$	1201	1.72
$\text{NdFe}_{10}\text{Co}(8f)_{1.6}\text{As}_{0.4}$	1200	1.69
$\text{NdFe}_{10}\text{Co}(8f)_{1.8}\text{Ge}_{0.2}$	1199	1.71
$\text{NdFe}_{10}\text{Co}(8f)_{1.4}\text{As}_{0.6}$	1198	1.65
$\text{NdFe}_{10}\text{Co}(8f)_{1.2}\text{As}_{0.8}$	1198	1.62
$\text{NdFe}_{10}\text{Co}(8f)_{2.0}$	1198	1.76
$\text{NdFe}_{10}\text{Co}(8f)_{1.6}\text{Ge}_{0.2}\text{As}_{0.2}$	1197	1.68
$\text{NdFe}_{10}\text{Co}(8f)\text{As}$	1197	1.59
$\text{NdFe}_{10}\text{Co}(8f)_{1.6}\text{Ge}_{0.4}$	1195	1.68
$\text{NdFe}_{10}\text{Co}(8f)_{0.8}\text{Ge}_{1.2}$	1195	1.56
$\text{NdFe}_{12}$	881	1.73

reduce the amount of Co, which is an expensive element, without sacrificing the Curie temperature.

#### IV. CONCLUSION

In this paper, we have discussed the effects of various dopants (K-Br) on the magnetism of  $\text{NdFe}_{12}$ . We first investigated doping with a single dopant at an infinitesimal concentration, then extended the analysis to finite concentrations of selected dopants. We have demonstrated

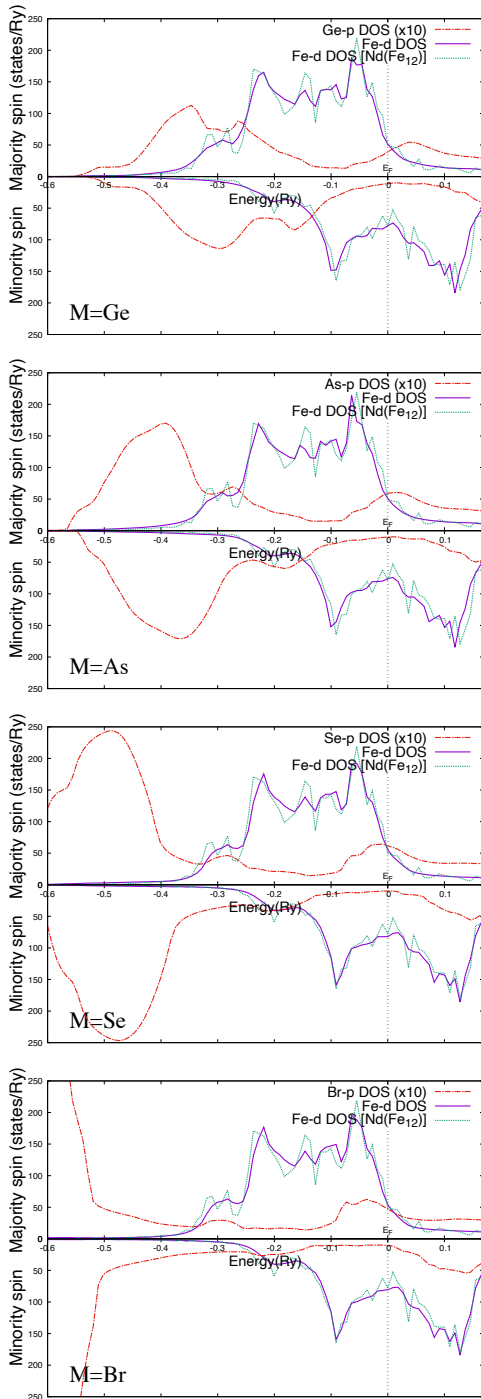


FIG. 7. Partial DOSs for the Fe d orbitals and M p orbitals (multiplied by ten) of the 8f-doped  $\text{Nd}(\text{Fe}_{11}\text{M})$  systems ( $\text{M}=\text{Ge}, \text{As}, \text{Se}, \text{or Br}$ ).

the potential of As and Ge in enhancing the Curie temperature and discussed the origin of this enhancement in terms of the interaction between the Fe 3d and M 4p electrons. These results were used to screen the dopants prior to further optimization using a wider search space that allowed for simultaneous doping. We found that co-

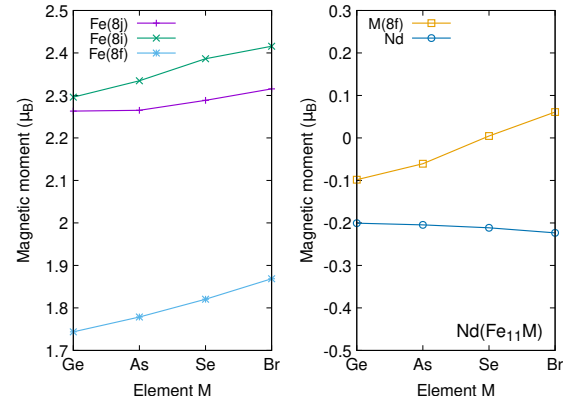


FIG. 8. Local magnetic moments in 8f-doped  $\text{Nd}(\text{Fe}_{11}\text{M})$  ( $\text{M}=\text{Ge}, \text{As}, \text{Se}, \text{or Br}$ ).

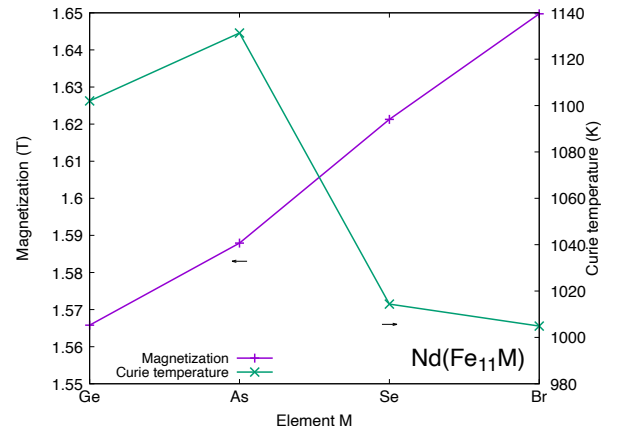


FIG. 9. Magnetization and Curie temperature for 8f-doped  $\text{Nd}(\text{Fe}_{11}\text{M})$  ( $\text{M}=\text{Ge}, \text{As}, \text{Se}, \text{or Br}$ ).

doping with As, Ge, and Co has the potential to enhance the Curie temperature more efficiently than doping with Co alone. The results also indicate that doping with As and Ge can reduce the amount of Co, which is a scarce element, without reducing the Curie temperature.

## ACKNOWLEDGMENT

This work was supported by a project (JPNP20019) commissioned by the New Energy and Industrial Technology Development Organization (NEDO), the Elements Strategy Initiative Center for Magnetic Materials (ESICMM, Grant Number JPMXP0112101004), and the “Program for Promoting Researches on the Supercomputer Fugaku” (DPMSD) by MEXT. The calculations were conducted in part using the facilities of the Supercomputer Center at the Institute for Solid State Physics, University of Tokyo, the supercomputer of the Academic Center for Computing and Media Studies (ACCMS), Kyoto University, and the supercomputer Fugaku provided by the RIKEN Center for Computational Science

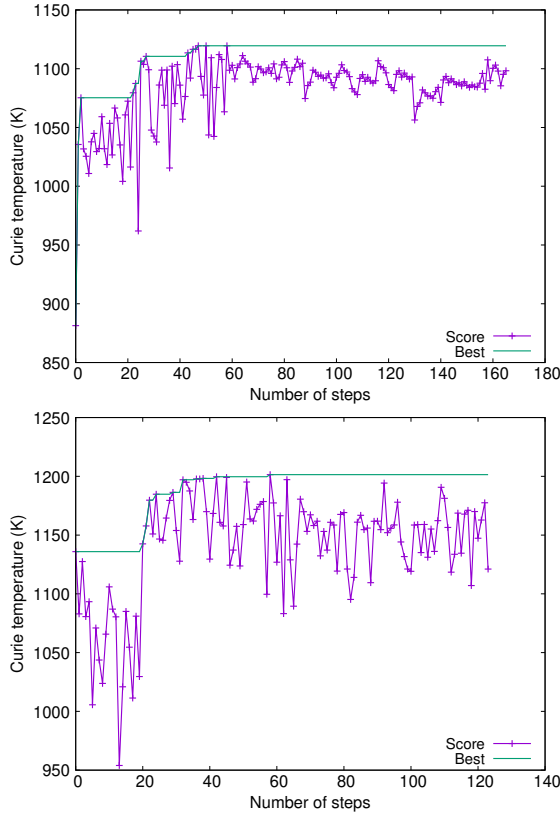


FIG. 10. Values of the Curie temperature at each optimization step for list (A) (top) and list (B) (bottom).

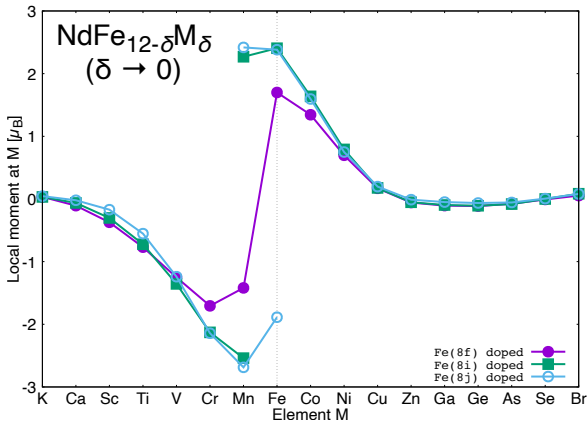


FIG. 11. Local magnetic moments of  $M$  for  $\text{Nd}(\text{Fe}_{12-\delta}\text{M}_\delta)$  in the dilute limit,  $\delta \rightarrow 0$ .

through the HPCI System Research Project (Project ID: hp200125, hp210179).

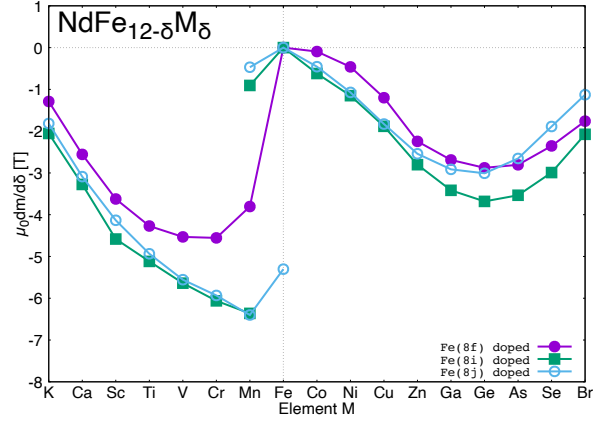


FIG. 12. Derivative of the magnetization for  $\text{Nd}(\text{Fe}_{12-\delta}\text{M}_\delta)$  with respect to  $\delta$  in the dilute limit,  $\delta \rightarrow 0$ .

## Appendix A: Magnetic moment

### 1. $\text{NdFe}_{12-\delta}\text{M}_\delta$ ( $\delta \ll 1$ )

In this subsection, we present results for the magnetic moments in  $\text{NdFe}_{12-\delta}\text{M}_\delta$  ( $\delta \ll 1$ ). In Fig. 11, the local magnetic moments of  $M$  at the 8f, 8i, and 8j sites are shown. Parallel and antiparallel solutions coexist only in the cases of Fe(8i) doping with  $M = \text{Mn}$  and Fe(8j) doping with  $M = \text{Fe}$  and Mn. Irrespective of the choice of doping site, the stable solution was antiparallel for  $M = \text{Mn}$  and parallel for  $M = \text{Fe}$ .

It has been discussed in the context of magnetic impurity problems that metastable states are more likely to exist when the host has a small magnetic moment.[26] The host is identical in our calculations, but the existence of a metastable state depends on the doping site. The calculated local moments of Fe in  $\text{NdFe}_{12}$  were  $1.70 \mu_B$  at the 8f site,  $2.41 \mu_B$  at the 8i site, and  $2.38 \mu_B$  at the 8j site. Therefore, the Fe moments surrounding the 8f site were larger than those surrounding the other sites. This leads to the non-existence of the metastable state in the range of our calculations for 8f doping.

Let us next consider the rate of change of the magnetization  $m$  with respect to the concentration. Figure 12 shows the derivative of the magnetization,  $\left. \frac{dm}{d\delta} \right|_{\delta=0}$ , as a function of the dopant  $M$ . The magnetic moment decreases upon doping. In the case of the elements to the left of the plot (K–Fe), this is because the local moment of  $M$  is antiparallel to the host. In the case of those to the right of the plot (Mn–Br), this is because the local moment of the replacing element is smaller than that of the replaced Fe, which we call the direct contribution in DID analysis. However, this decrease is suppressed for  $M = \text{Ge} - \text{Br}$ , even though the local moment of  $M$  is almost zero. This indicates that these elements have an indirect effect on the magnetic moment which is proportional to the first order of the concentration and counteracts the direct effect.

## 2. Finite amount of $M$

Figure 13 shows the results for the magnetization of  $\text{NdFe}_{12-x}M_x$  ( $0 \leq x \leq 2$ ). In the cases of  $M=\text{V}$  and  $\text{Cr}$ , the magnetic moment of  $M$  is antiparallel to the host

magnetization, and the total magnetization sharply decreases as the concentration of  $M$  increases. In the cases of  $M=\text{Co}$  and  $\text{Ni}$ , the magnetic moment of  $M$  is parallel to the host, and the total magnetization is retained at higher concentrations. Because  $\text{Ge}$  and  $\text{As}$  are nonmagnetic, the decrease in the total magnetization is moderate compared with the cases of  $M=\text{Ge}$  and  $\text{As}$ .

- 
- [1] Y. Hirayama, Y. Takahashi, S. Hirosawa, K. Hono,  $\text{NdFe}_{12} \text{N}_x$  hard-magnetic compound with high magnetization and anisotropy field, *Scripta Materialia* 95 (2015) 70–72.  
URL <http://www.sciencedirect.com/science/article/pii/S1359646214004163>
- [2] Y. Hirayama, T. Miyake, K. Hono, Rare-earth lean hard magnet compound  $\text{ndfe}_{12}\text{n}$ , *JOM* 67 (6) (2015) 1344–1349.
- [3] K. Ohashi, T. Yokoyama, R. Osugi, Y. Tawara, The magnetic and structural properties of R-Ti-Fe ternary compounds, *IEEE transactions on magnetics* 23 (5) (1987) 3101–3103.
- [4] K. Ohashi, Y. Tawara, R. Osugi, J. Sakurai, Y. Komura, Identification of the intermetallic compound consisting of sm, ti, fe, *Journal of the Less Common Metals* 139 (2) (1988) L1–L5.  
URL <http://www.sciencedirect.com/science/article/pii/0022508888900203>
- [5] Y. Harashima, K. Terakura, H. Kino, S. Ishibashi, T. Miyake, First-principles study on stability and magnetism of  $\text{NdFe}_{11}M$  and  $\text{NdFe}_{11}MN$  for  $M=\text{Ti, V, Cr, Mn, Fe, Co, Ni, Cu, Zn}$ , arXiv preprint arXiv:1609.07227 (2016).
- [6] Y. Hirayama, Y. K. Takahashi, S. Hirosawa, K. Hono, Intrinsic hard magnetic properties of  $\text{Sm}(\text{Fe}_{1-x}\text{Co}_x)_{12}$  compound with the  $\text{ThMn}_{12}$  structure, *Scripta Materialia* 138 (2017) 62–65.
- [7] T. Fukazawa, H. Akai, Y. Harashima, T. Miyake, First-principles study of intersite magnetic couplings and Curie temperature in  $\text{RFe}_{12-x}\text{Cr}_x$  ( $\text{R} = \text{Y, Nd, Sm}$ ), *Journal of Physical Society of Japan* 87 (4) (2018) 044706.
- [8] A. Schönhöbel, R. Madugundo, O. Y. Vekilova, O. Eriksson, H. C. Herper, J. Barandiarán, G. Hadjipanayis, Intrinsic magnetic properties of  $\text{smfe}_{12-x}\text{v}_x$  alloys with reduced v-concentration, *Journal of Alloys and Compounds* 786 (2019) 969–974.
- [9] T. Fukazawa, Y. Harashima, Z. Hou, T. Miyake, Bayesian optimization of chemical composition: A comprehensive framework and its application to  $\text{RFe}_{12}$ -type magnet compounds, *Physical Review Materials* 3 (5) (2019) 053807.
- [10] P. Hohenberg, W. Kohn, Inhomogeneous electron gas, *Physical Review* 136 (3B) (1964) B864.
- [11] W. Kohn, L. J. Sham, Self-consistent equations including exchange and correlation effects, *Physical Review* 140 (4A) (1965) A1133.
- [12] J. Korringa, On the calculation of the energy of a bloch wave in a metal, *Physica* 13 (6-7) (1947) 392–400.
- [13] W. Kohn, N. Rostoker, Solution of the schrödinger equation in periodic lattices with an application to metallic lithium, *Phys. Rev.* 94 (1954) 1111–1120. doi:10.1103/PhysRev.94.1111.  
URL <http://link.aps.org/doi/10.1103/PhysRev.94.1111>
- [14] J. P. Perdew, A. Zunger, Self-interaction correction to density-functional approximations for many-electron systems, *Phys. Rev. B* 23 (1981) 5048–5079. doi:10.1103/PhysRevB.23.5048.  
URL <http://link.aps.org/doi/10.1103/PhysRevB.23.5048>
- [15] P. Soven, Coherent-potential model of substitutional disordered alloys, *Physical Review* 156 (3) (1967) 809.
- [16] P. Soven, Application of the coherent potential approximation to a system of muffin-tin potentials, *Physical Review B* 2 (12) (1970) 4715.
- [17] H. Shiba, A reformulation of the coherent potential approximation and its applications, *Progress of Theoretical Physics* 46 (1) (1971) 77–94.
- [18] Y. Harashima, K. Terakura, H. Kino, S. Ishibashi, T. Miyake, First-principles study of structural and magnetic properties of  $\text{r}(\text{fe, ti})_{12}$  and  $\text{r}(\text{fe, ti})_{12}\text{n}$  ( $\text{r}=\text{nd, sm, y}$ ), in: *Proceedings of Computational Science Workshop 2014 (CSW2014)*, Vol. 5 of *JPS Conference Proceedings*, 2015, p. 1021.  
URL <http://journals.jps.jp/doi/abs/10.7566/JPSCP.5.011021>
- [19] A. I. Liechtenstein, M. Katsnelson, V. Antropov, V. Gubanov, Local spin density functional approach to the theory of exchange interactions in ferromagnetic metals and alloys, *Journal of Magnetism and Magnetic Materials* 67 (1) (1987) 65–74.
- [20] T. Fukazawa, H. Akai, Y. Harashima, T. Miyake, Curie temperature of  $\text{Sm}_2\text{Fe}_{17}$  and  $\text{Nd}_2\text{Fe}_{14}\text{B}$ : a first-principles study, *IEEE Transaction on Magnetics* (in press).  
URL <https://ieeexplore.ieee.org/document/8653984>
- [21] T. Ueno, T. D. Rhone, Z. Hou, T. Mizoguchi, K. Tsuda, COMBO: An efficient Bayesian optimization library for materials science, *Materials discovery* 4 (2016) 18–21.
- [22] COMMon Bayesian Optimization Library (COMBO), <https://github.com/tsudalab/combo>.  
URL <https://github.com/tsudalab/combo>
- [23] J. Kanamori, Interplay between electronic structure and correlation through the sd mixing in transition metal systems, *Progress of Theoretical Physics Supplement* 101 (1990) 1–10.
- [24] M. Ogura, H. Akai, J. Kanamori, Enhancement of Magnetism of Fe by Cr and V, *Journal of the Physical Society of Japan* 80 (10) (2011) 104711.
- [25] Y. Harashima, K. Terakura, H. Kino, S. Ishibashi, T. Miyake, Nitrogen as the best interstitial dopant among  $X=\text{B, C, N, O}$ , and F for strong permanent magnet  $\text{NdFe}_{11}\text{TiX}$ : First-principles study, *Phys. Rev.*

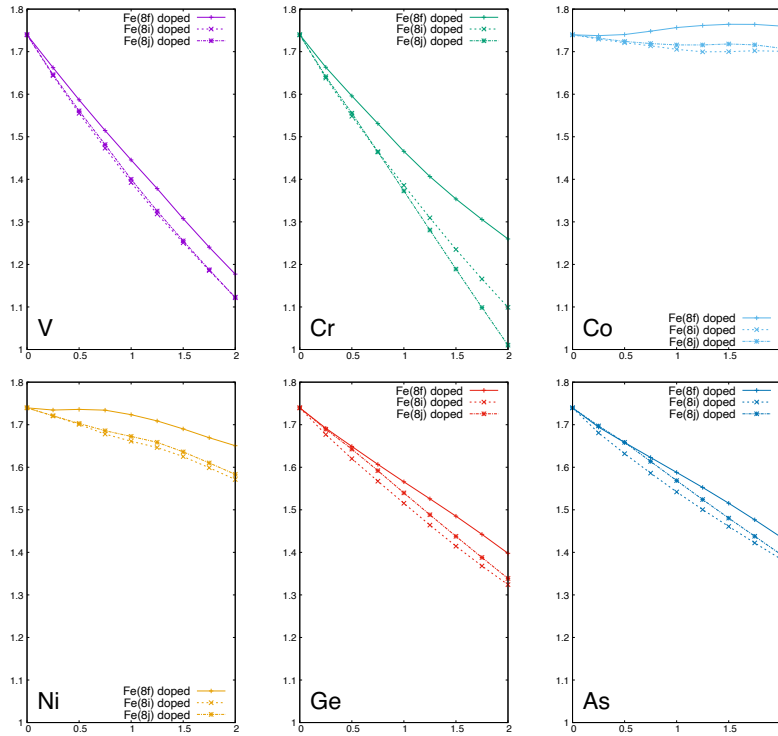


FIG. 13. Magnetization of  $\text{Nd}(\text{Fe}_{12-x}\text{M}_x)$  ( $M=\text{V}, \text{Cr}, \text{Co}, \text{Ni}, \text{Ge}, \text{or As}$ ) with finite concentrations  $x$  in the range of  $0 \leq x \leq 2$ .

B 92 (2015) 184426. doi:10.1103/PhysRevB.92.184426.  
 URL <http://link.aps.org/doi/10.1103/PhysRevB.92.184426>

[26] H. Akai, M. Akai, S. Blügel, B. Drittler, H. Ebert, K. Terakura, R. Zeller, P. Dederichs, Theory of hyperfine inter-

actions in metals, Progress of Theoretical Physics Supplement 101 (1990) 11–77.

URL <http://ptps.oxfordjournals.org/content/101/11.short>